AIAA 1999-0134

DRAG REDUCTION EXPERIMENTS USING BOUNDARY LAYER HEATING

Brian R. Kramer, Brooke C. Smith, Joseph P. Heid
Eidetics Corporation
Torrance, CA

Gregory K. Noffz, David M. Richwine
NASA Dryden Flight Research Center
Edwards, CA

Terry Ng
University of Toledo
Toldeo, OH

37th AIAA Aerospace Sciences Meeting & Exhibit
January 1999 / Reno, NV

AIAA-99-0134

DRAG REDUCTION EXPERIMENTS USING BOUNDARY LAYER HEATING

Brian R. Kramer*, Brooke C. Smith†, Joseph P. Heid‡
Eidetics Corporation, Torrance, California

Gregory K. Noffz§, David M. Richwine¶
NASA Dryden Flight Research Center
Edwards, California

Terry Ng#
University of Toledo
Toledo, Ohio

ABSTRACT

A new technique for reducing the drag of existing aircraft configurations was investigated. Heating the surface under a turbulent boundary layer reduces the turbulent skin friction. An experimental program was conducted to determine the feasability of applying this technology to military and commercial aircraft. Three different experimental investigations were conducted to measure the extent of the drag reduction. The first experiment was a low speed wind tunnel test. Very significant drag reduction was measured while only heating the forward portion of the wind tunnel model. In order to determine the effects of higher Mach and Reynolds number, a flight test program was conducted using the NASA Dryden F-15B Flight Test Fixture. The experiment measured the skin friction over a flat plate using a momentum deficit technique. The magnitude of the drag reduction was less than measured in the wind tunnel, but showed a trend of increasing effectiveness with decreasing Reynolds number. The third experiment confirmed the overall drag reduction on a business jet class aircraft. This work has shown that significant drag savings can be achieved using boundary layer heating.

NOMENCLATURE

a	Local speed of sound, ft/sec
C_f	Friction coefficient
D_f	Drag due to skin friction
γ	Specific heat ratio
g	Acceleration of gravity, ft/s^2
K_T	Total temperature correction factor
μ	Dynamic viscosity, lb-sec/ft^2
M	Mach number
P_T	Total pressure, lb/ft^2
P	Static pressure, lb/ft^2
ρ	Density, slugs/ft^3
R	Gas constant, air, 53.3 ft-lb$_f$/(lb$_m$-°R)
θ	Momentum thickness, ft
T	Static temperature, deg. Rankine
TR	Temperature ratio
T_T	Total temperature, deg. Rankine
u	Local velocity, ft/sec
U	Free stream velocity, ft/sec
x	Axial location, ft
y	Boundary layer height, ft

INTRODUCTION

The benefits of reducing the drag of either a new or existing aircraft configuration are obvious. An aircraft's endurance is directly proportional to its lift to drag ratio. Decreased drag also translates into faster top speed, quicker acceleration, shorter take-off distances and lower direct operating costs in the form of fuel savings. In order to project military air power, or on the commercial side, receive better range and fuel economy, reducing drag during the cruise portion of a flight is critical.

During cruise, the drag of the aircraft primarily comes from profile drag (skin friction), induced drag (drag due to lift), compressibility drag, separation drag and interference drag. Of these, skin friction (from the "wetted" elements of the aircraft) typically accounts for more than 50% of the total. In order to decrease the skin friction of an aircraft, many methods have been successfully employed that delay the transition of the

* Director, Advanced Technology Development. Senior Member AIAA
† Chief Scientist. Senior Member AIAA
‡ Engineering Specialist.
§ Aerospace Engineer
¶ Aerospace Engineer. Member AIAA
# Professor. Senior Member AIAA

boundary layer from laminar to turbulent. These methods fall into three categories: Natural Laminar Flow (NLF), Laminar Flow Control (LFC), and a combination of the two referred to as Hybrid Laminar Flow Control (HLFC). A major drawback to this approach to drag reduction, is the extreme difficulty in retrofitting an existing aircraft to incorporate these drag reducing techniques. There are also many maintainability issues concerning bug / bird strikes and general contamination of the surface. This approach is also only effective on wing and tail surfaces because the length of most (particularly transport) aircraft fuselages cause the Reynolds number to be far too great (can be over 300 million) to maintain laminar flow. Another approach to reducing the total aircraft drag is to reduce the existing turbulent skin friction drag. A well-known method for doing this is with riblets. Riblets are very small v-shaped grooves that are attached to, or manufactured into, the aircraft's skin, and are aligned in the direction of the flow. Riblets have the advantage of providing significant drag reduction (≈4%) while being simple to apply to an existing aircraft as well as a new design. Perhaps the greatest single reason that riblets have not found wide spread acceptance in commercial aviation is the issue of maintainability. In order to function correctly, the grooves in the riblet material must be kept clean. This could be a real problem for aircraft that spend most of their flight time at lower altitudes.

The current research uses active surface heating in the turbulent regions of the aircraft's boundary layer. When heat is added to the turbulent boundary layer, the skin friction is reduced roughly as a function of the ratio of the skin temperature to the ambient temperature. The benefit of wall heating on the skin friction drag, which is caused by the difference in viscosity and density of a fluid when it is heated, can easily be seen with a simple calculation of skin friction as a function of temperature[1]:

$$D_f \propto \mu^{\left(\frac{1}{6}\right)} \rho^{\left(\frac{5}{6}\right)}$$

define temperature ratio as:

$$TR = \frac{T_{BL}}{T_\infty}$$

$$\frac{\rho_{BL}}{\rho_\infty} = \frac{1}{TR}$$

$$\frac{\mu_{BL}}{\mu_\infty} \approx TR$$

therefore:

$$\frac{D_{fBL}}{D_{f\infty}} \approx TR^{\left(\frac{1}{6}\right)} TR^{-\left(\frac{5}{6}\right)} = TR^{-\left(\frac{2}{3}\right)}$$

A series of experiments were conducted to determine the feasibility of using boundary layer heating to reduce skin friction drag on an aircraft. The first experiment was a low speed wind tunnel test, sponsored through an SBIR I program by NASA Ames. This experiment produced very promising results, but at very low Reynolds and Mach numbers. The next two experiments were sponsored by NASA Dryden Flight Research Center under an SBIR Phase II contract. The initial experiment was conducted at representative flight Mach and Reynolds numbers using the F-15B Flight Test Fixture (FTF). The final flight experiment was conducted using a Sabreliner business jet (T-39) at the same flight conditions. The results from these experiments were then used to evaluate the feasibility of such a system for use by the airlines or the military.

LOW SPEED WIND TUNNEL TEST

The first experiment was conducted in the University of Toledo 3'x3' Low Speed Wind Tunnel. The drag force generated on a model of this scale, in a low speed tunnel, can be expected to be quite small. This can be a major problem for most typical wind tunnel balances. However, Eidetics has previously developed a semi-conductor strain gage balance with enough sensitivity to be used in a low speed (1 ft/sec) water tunnel[2, 3]. The drag force expected on the wind tunnel model was extremely small which necessitated the use of semi-conductor strain gages, which are 50 to 100 times as sensitive as either wire or foil strain gages. A simple bending beam design was used for the drag balance. An air bearing and load cell were used as a back-up system.

A new support scheme was devised in which the forward support of the balance was a rotating pin and the aft support was a double-pinned mount (to approximate a free sliding support). The front pin allows only an axial force to be transferred to the balance without a moment. This allows the front and rear supports to grow in length without loading the balance. The double-pinned aft support allows the model to grow in length without applying a load to the balance. The actual mechanization of this is shown in Fig. 1. The hinge pieces were carefully machined and the design proved very efficient in isolating any thermal effects from the balance readings.

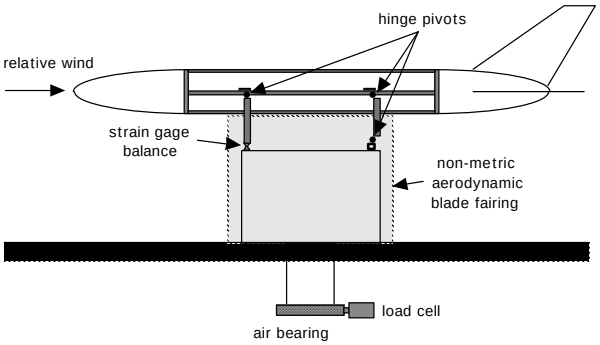

Figure 1: Low Speed Wind Tunnel Test Layout

Wind Tunnel Model

The aircraft modeled for the wind tunnel represents either a military or a commercial transport configuration. As shown in Figure 1, the model has a fineness ratio of approximately 10, which allows comparison with Lin's computational work[4]. This type of aircraft has a very large potential market for an effective and inexpensive "after-market" drag reduction system. A transonic transport aircraft also has a larger portion of its drag produced by skin friction than a fighter does where compressibility, interference and separation drag are more prominent.

Three different aft end configurations were tested. First, a non-tapered aft end was tested with heating strips covering its entire length. This shape was less susceptible to changes in separation location when heating was applied. The second aft end had a tapered shape that was identical to the nose cone. Because of modeling difficulties, this aft end was not heated, but the shape was more representative of a true aircraft aft fuselage. Finally, the model was run without an aft end piece, which provided a blunt aft body like the first configuration, but a shorter overall length than the other two.

Because the ambient temperature in the wind tunnel was approximately 80° F (540° R), a fairly high temperature source was needed. An actual aircraft will operate at a much lower ambient temperature. The heater elements were molded directly into a section of the fuselage skin. Silicon rubber heaters were the most effective and had the least problem with debonding.

In the wind tunnel, with sea level air density, the maximum temperature achieved was approximately 240°F. This corresponds to a temperature ratio of approximately 1.25 in the wind tunnel.

Effect of Single Heater Element

The effect of applying heat to the skin surface was measured for several configurations. The first configuration was the most representative of a real fuselage, with both a tapered nose and a tapered aft body. Figure 2 shows the relative effectiveness of the five single heaters. As was expected, the heat was most effective when it was applied on the forward part of the body, and becomes less effective as the application point was moved aft. This was because once the properties of the fluid were modified by the heating, that same fluid was convected down the body and reduced the skin friction on the region downstream of the heat source. Therefore, although the skin friction reduction was locally the same for all of the elements, the forward location allowed more area downstream to be effected.

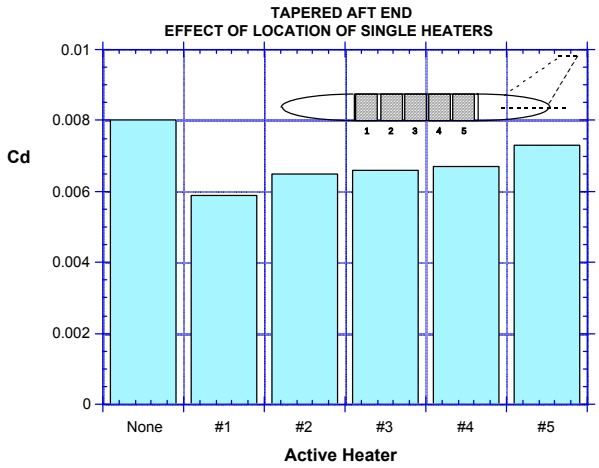

Figure 2: Single Heater Effect

Effect of Heater Pairs

When pairs of heaters were considered (Fig. 3), the results were similar. Based on the data from the single heaters, it was expected that the pair of elements 1 and 2 would provide the most benefit, and that as the pairs were moved aft the benefit would decrease. However, the pair of elements 2 and 3 were about as effective (slightly better in fact). Elements 3 and 4 were considerably less effective, however. An attempt was made to provide the most effective combination by leaving a gap between the heaters. It was hoped that the effect of heater 1 would carry downstream and then be reinforced by element 3 and yield a net benefit equal to heating elements 1,2 and 3 at 2/3 of the cost. It turns out that the effect was very close to that achieved by heating all three elements (see Fig. 4), but that was no better than just heating elements 1 and 2. Perhaps an optimum could be found by heating elements 1 and 5, or 1 and 4. Since these particular configurations were not run, it was left to future optimization work.

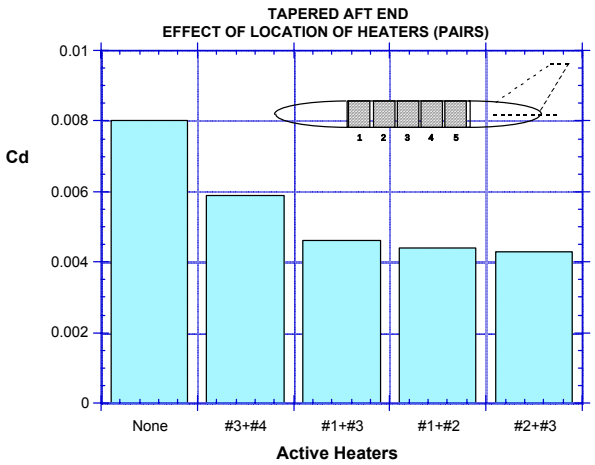

Figure 3: Effect of Heater Pair Location

Effect of Multiple Heater Elements - Tapered Aft Body

Figure 4 shows the effect of starting at the front of the model and progressively adding heaters aft. As expected, when all of the elements are heated, the drag reduction was the greatest. However, this was at the cost of electrical energy and weight.

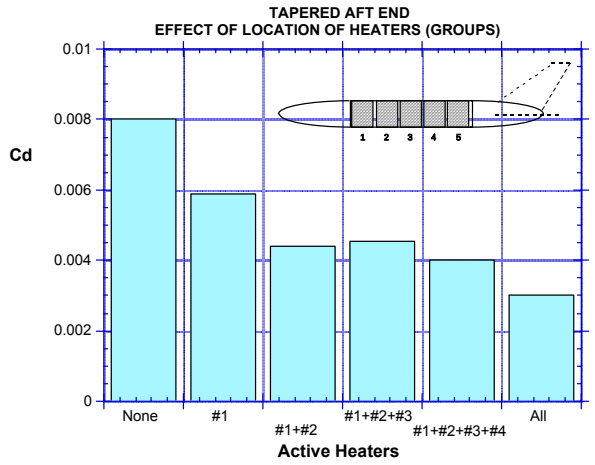

Figure 4: Effect of Heater Length - Tapered Aft Body

Effect of Multiple Heater Elements - Truncated Aft Bodies

Because the drag reduction measured was more than that predicted, the model was run in two additional configurations to try to rule out a change in separation location. Because the two additional configuration both had blunt aft ends, it was assumed that the entire base area flow was separated, and didn't change (become less separated) when heat was applied. Both the short and long blunt fuselages, in Figs. 5 and 6, show the same type of trend in drag reduction with additional heat addition.

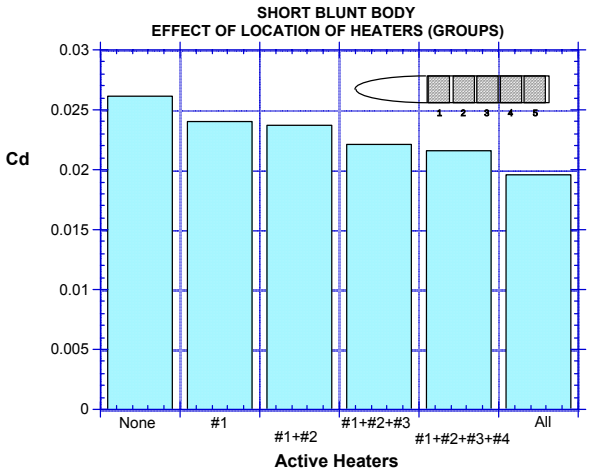

Figure 5: Effect of Heater Length - Short Blunt Body

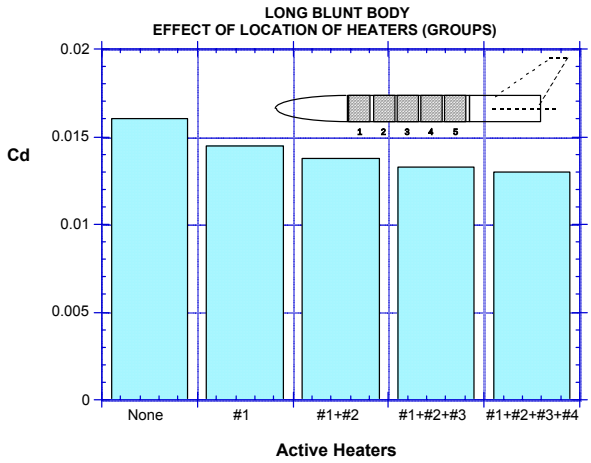

Figure 6: Effect of Heater Length - Long Blunt Body

Determination of Skin Friction Coefficient

In order to determine if the skin friction coefficients were similar in all cases, an analysis was conducted to break out the components of the drag. It should be noted that the drag coefficients used are referenced to wetted area so the short fuselage data was reduced with a much smaller area term. The following equations define the drag build up:

$$TotalDrag = BaseDrag + SkinFrictionDrag + OtherDrag$$

$$= BaseDrag + (UnheatedSkinFriction + HeatedSkinFriction) + Other$$

$$C_{D_{TOTAL}} \bar{q} S_{REF} = C_{D_{BASE}} \bar{q} S_{BASE} + C_{D_{COLD}} \bar{q} S_{COLD} + C_{D_{HOT}} \bar{q} S_{HOT} + Other$$

$$C_{D_{TOTAL}} = C_{D_{BASE}} \frac{S_{BASE}}{S_{REF}} + C_{D_{COLD}} \frac{S_{COLD}}{S_{REF}} + C_{D_{HOT}} \frac{S_{HOT}}{S_{REF}} + C_{D_{OTHER}}$$

Figure 7 shows the drag build up for the case of heater element 1 alone. The base drag term was applied to the entire diameter of the model for the two truncated models, and to the rounded off area (ball) of the tapered aft body. The "cold" skin friction coefficient was calculated for the case of the unheated model, and then used as a constant (0.0085) for all subsequent calculations. The average value for the heated skin friction falls to 0.0057, and shows very good agreement for all three configurations.

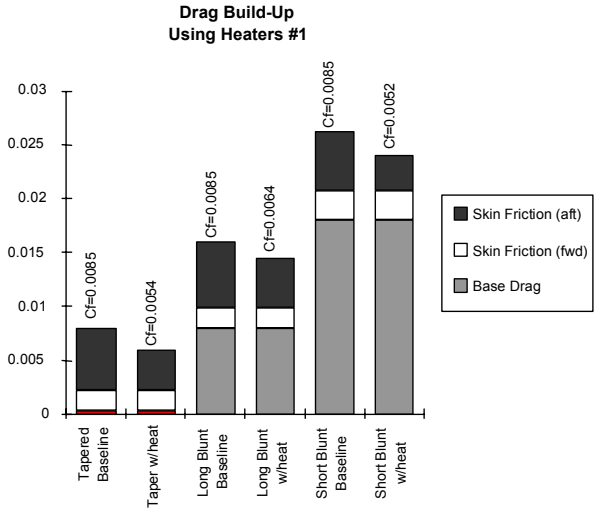

Figure 7: Drag Build-Up Heater #1

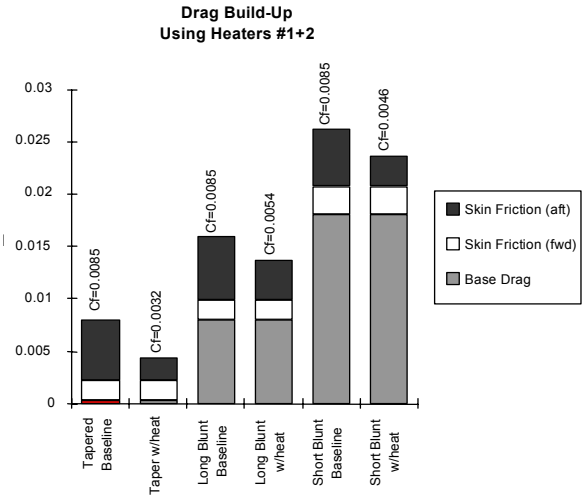

Figure 8: Drag Build-Up Heaters #1 and #2

Figures 7-10 show the various other combinations of heater elements. In general, the more elements that were heated, the lower the heated skin friction coefficient value became. The conclusion from this analysis was that a change in separation location does not appear to be the cause of the large drag reduction.

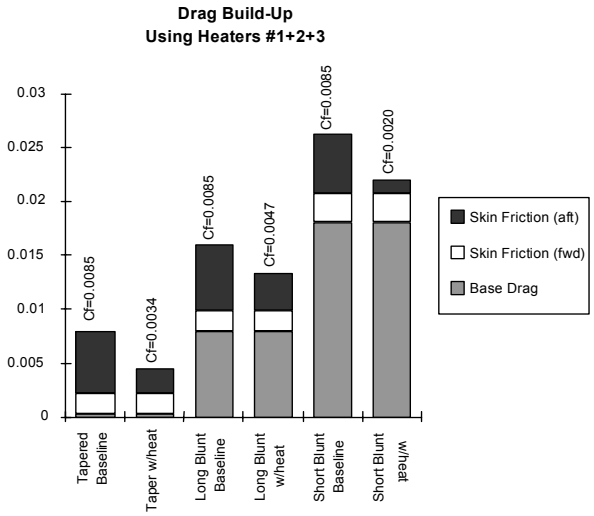

Figure 9: Drag Build-Up Heaters #1, #2 and #3

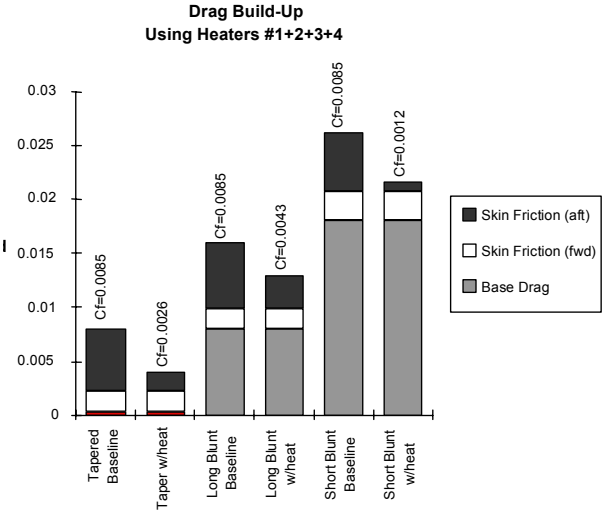

Figure 10: Drag Build-Up Heaters #1, #2, #3 and #4

Comparison to Previous Computational Study

The results from the wind tunnel test were compared not only to the preliminary estimates that were made based on Hoerner's simplified relationships, but also with Ref. 4, the work of Lin and Ash entitled "Wall Temperature Control of Low-Speed Body Drag." Lin and Ash's work was entirely computational, with no experimental verification. This work was performed on a fineness ratio 10.8 body at a Mach number of 0.2 and

a Reynolds number of 1.37 million/ft (148 million based on fuselage length). At a temperature ratio of 2, with the entire body heated, a 20% drag reduction was calculated. When only the front half of the model was heated, a 13% drag reduction was calculated, which demonstrates that their code took into account the benefit of the heat being convected downstream.

The current experimental data was measured on a fineness ratio 9.4 body at Mach 0.06 and a Reynolds number of 0.4 million/ft (1.6 million based on fuselage length). The drag reduction measured was 26% when heat was added at a temperature ratio of 1.28 for 8.5% of the body length (strip #1).

The reason for the increased drag reduction is most likely due to a Reynolds number effect. For example, the laminar sub-layer of the boundary layer may be thickened with the application of heat and cause some of the surface roughness to be hidden in the boundary layer. This provided the motivation to perform a high Mach and Reynolds number test.

F-15 FLIGHT TEST FIXTURE EXPERIMENT

The second experiment was performed on the NASA Dryden F-15B Flight Test Fixture. This experiment, and the third flight test were sponsored by NASA Dryden in a Phase II SBIR. The fixture is essentially a wind tunnel in the sky that can provide true flight Mach and Reynolds numbers. The FTF (Fig. 11) is a flat plate with an elliptical leading edge, and a rear fairing (not shown) that provides a shallow closure angle. The two lower panels on the FTF are replaceable with those specific to an experiment, while the upper area is hollow and can carry instrumentation. The FTF was carried underneath the F-15B on its centerline pylon station. Figure 12 shows the boundary layer heat experiment in flight with the pressure and temperature rakes mounted in the aft position.

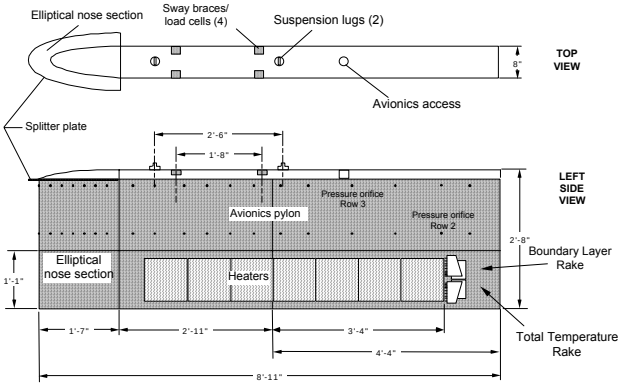

Figure 11: F-15B Flight Test Fixture

Flight Conditions and Instrumentation

The flight conditions of interest for this experiment were altitudes of 25,000, 30,000, and 35,000 feet with Mach numbers of 0.70, 0.75 and 0.80. The data collected for this experiment included all of the typical flight parameters as well as static pressure and temperature at various positions along the FTF and the heater power consumed. In addition, a total pressure boundary layer rake and a pseudo total temperature rake could be positioned at either the leading edge or trailing edge of the heated section. As in the wind tunnel test, the heaters were individually controlled so that effects of length and position could be examined.

Figure 12: Boundary Layer Heating Experiment in Flight

Data Reduction

The primary goal of this experiment was to measure the skin friction associated with the FTF panels, with and without the electric heaters activated. The data reduction for this experiment was similar to that used by Fanny Zuniga et al during a Riblets experiment[5] in 1992. The approach was to use a momentum deficit technique. The primary difference between the Riblets data reduction and that proposed for the present experiment, was that a constant Total Temperature could be assumed for the Riblets work, but not for the current study.

A new total temperature rake was designed and built that used thermistors mounted in stainless steel tubes. A recovery factor for each of the individual temperature sensors was computed by comparing it to the known FTF total temperature reading during a non-heated flight.

The local mach number was computed for each rake station by using the local total pressure from the rake and an average of the 3 static pressures at the base of the rake.

$$M_y = \sqrt{\frac{2}{\gamma - 1}\left[\left(\frac{P_{T_y}}{P_{rake}}\right)^{\frac{\gamma-1}{\gamma}} - 1\right]}$$

Next, the static temperature was determined using the mach numbers calculated above for each rake station, and the total temperatures measured from the total temperature rake at the same stations. Note that K_{Ty} is the recovery factor for each total temperature probe.

$$T_y = \frac{T_{T_y}\left(K_{T_T}\right)}{\left[1 + \left(\frac{\gamma - 1}{2}\right)M_y^{\,2}\right]}$$

Likewise, the local density, local speed of sound and local velocity was calculated for each rake station.

$$\rho_y = \frac{P_{rake}}{RgT_y}$$

$$a_y = \sqrt{\gamma RgT_y}$$

$$u_y = a_y M_y$$

Finally, the boundary layer momentum thickness was calculated. Each rake position was assigned the appropriate delta height for the integration.

$$\theta = \int_0^\infty \left[\frac{\rho_y u_y}{\rho U}\left(1 - \frac{u_y}{U}\right)\right] dy$$

Then, the skin friction coefficient was determined from the following equation that used the difference in momentum thickness between the forward and aft rake stations.

$$C_f = 2\frac{d\theta}{dx} = 2\left(\frac{\theta_2 - \theta_1}{x_2 - x_1}\right)$$

There were two primary differences between this approach and the one used for the Riblets experiment. First, the conditions at the forward rake station were measured instead of estimated with CFD. Secondly, the temperature profile was measured instead of assumed to be constant.

Results from FTF Experiment

Figure 13 shows a typical Total Temperature profile through the boundary layer for the heated and unheated cases. Notice that the recovery factor for each sensor forces it to match the total temperature. The recovery factors turned out to be rather small.

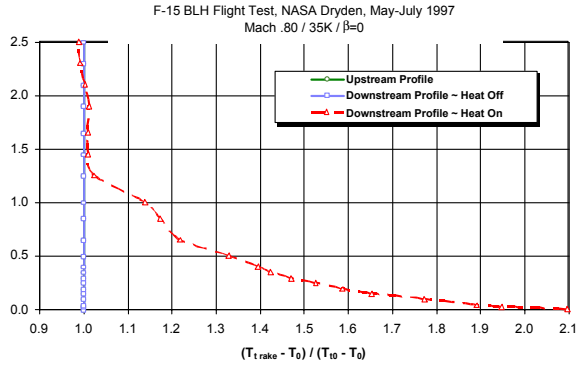

Figure 13: Boundary Layer Temperature Profile

Figure 14 shows a summary of all the flight conditions for the case when all of the heaters were activated. The greatest drag reduction occurred at the lowest speed, highest altitude case tested and was greater than 16%. It should be noted that only one power setting was available for the heaters, so the comparison is made for equal power, not for equal surface temperature. In Fig. 15, the drag reduction is plotted as a function of Reynolds number. The drag reduction was seen to increase as Reynolds number was decreased, which could explain the large drag reduction seen in the wind tunnel experiment.

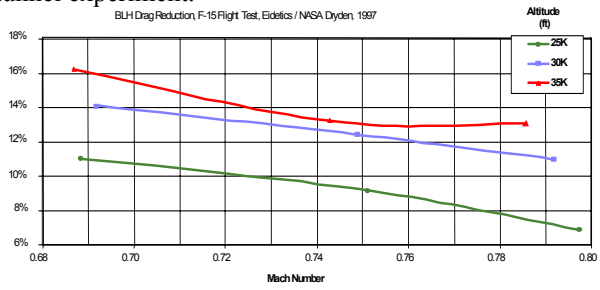

Figure 14: Drag Reduction as a Function of Altitude and Mach

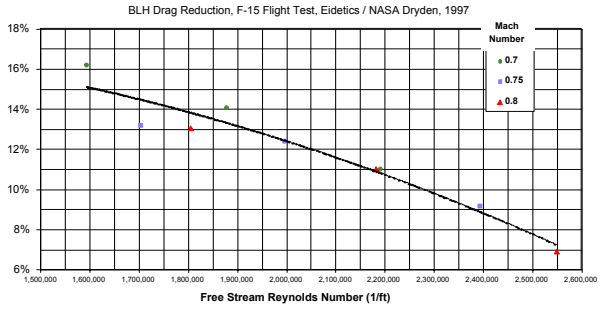

Figure 15: Drag Reduction as a Function of Reynolds Number

Figure 16 shows the drag reduction observed when a set of 3 heaters was used. The leading edge of the 3 heaters was moved from the very aft (rightmost bar) the very to front (the leftmost bar) of the FTF. The wind tunnel experiment lead us to expect that the more forward the heating, the more efficient it will be. This is because the local heating under the heated panels will be essentially the same, but the heat will convect downstream and provide some reduced benefit there as well. In the FTF experiment, as the heated area was moved forward, the drag reduction increased for the first 3 positions. After that point, moving further forward actually caused the drag increment to decrease. Even if the heat did not convect further downstream, the drag would be expected to hold constant. Since the drag was being measured indirectly with temperature and pressure rakes, it appears that the rakes did not capture the entire wake, and that some mixing from the sides occurred. To correct this, a wider band of heaters would have to be used. This effect should not be observed when using a 3 dimensional aircraft where the entire integrated effect can be measured.

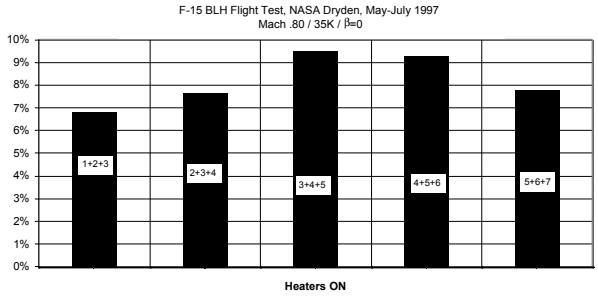

Figure 16: Effect of Position with 3 Heaters

BUSINESS JET FLIGHT TEST EXPERIMENT

The final set of flight tests in the series was performed using a North American T-39A aircraft (Sabreliner). The test article was a former USAF plane, which is now privately owned and operated as an experimental aircraft. The T-39A, shown in Fig. 17, was fitted with 48 etched foil electric heaters. The heaters will be attached to the forward portion of the fuselage in 4 bands, just aft of the pilot's windows. Each bank was individually controlled so that the temperature and the location of heating could be adjusted. The heaters were powered by a bank of sealed lead acid, deep cycle, batteries. The batteries were wired in series to provide a high voltage power source while keeping the current level lower so that smaller gauge wires could be used. The advantage of this kind of power source was that it was isolated from the engines, so the effect of boundary layer heating could be more directly correlated to the aircraft's performance.

Figure 17: T-39 Test Aircraft

An actual implementation of this system would likely not use batteries. For greater efficiency, it might be desirable to use generators driven by the engines, or other technique to supply heat to the boundary layer. Besides efficiency, another disadvantage of a battery driven system is the decline in voltage that is observed as power is drained. To avoid this problem, a "Buck" regulator system was built that is similar to those used in current electric car designs. This system allowed the test points to be completed with a power level that was consistent to within 1%. The batteries could be run at full power, on all 4 heater banks, for approximately 15 minutes before it was necessary to recharge the system. This allowed about 5 "power on" data points (more at lower power settings) without landing and recharging the batteries.

Flight Conditions and Instrumentation

The test points obtained were a subset of data points acquired on the F-15B FTF. Due to the increase in effectiveness at lower Reynolds numbers that was observed in the F-15B FTF experiment, a final test point was added at an altitude of 40,000 ft and Mach 0.70. The limiting factor on any of the slow speed points was the aircraft's performance. Fuel was off-loaded to obtain the final test condition.

Data was acquired using two PC based systems on board the aircraft. One system was used to measure the outside air data (altitude, airspeed, temperature etc.) and the engine parameters (pressure, exhaust gas temperature, RPM etc.). The second system provided the controls for the IGBT Buck Regulator and recorded the voltage, current and temperatures associated with heater panels.

Flight Procedure and Data Reduction

Measuring drag in a flight test is a very challenging task. For this experiment, there was less concern for the absolute drag level than for the incremental drag between heat on and heat off. The flight procedure that was used was to trim the aircraft at the desired altitude and speed, and then leave the throttles fixed. Baseline data was then taken in the trimmed condition. Power was then applied to the heaters while the pilots kept the aircraft straight and level. As the drag decreased, the aircraft sped up, and data was recorded at the new trim condition. The power was then turned off, and the return to baseline was recorded. At the simplest level, if the thrust is assumed constant, the ratio of the heat on versus heat off drag coefficients is simply the ratio of the dynamic pressure measured at each point:

$$T = D = C_{D1} q_1 S = C_{D2} q_2 S$$

$$\frac{C_{D2}}{C_{D1}} = \frac{q_1}{q_2}$$

Unfortunately, there are several over-simplifications with this approach[6]. The data reduction scheme used in this experiment corrected for the change in engine thrust[7], induced drag[8] due to the reduction in lift coefficient from the change in fuel weight and dynamic pressure. For the flight conditions evaluated, Mach effects and trim drag effects were negligible. Although data was recorded for nearly 5 minutes before, during and after heat was applied (for a total of 15 minutes), the aircraft did not appear to be completely trimmed. Part of the difficulty arose from the lack of an autopilot. In general, the pilots were able to hold plus or minus 50 feet in altitude. For this reason, a small correction was added to the data to remove the potential energy effects.

Results from T-39A Experiment

Although the Buck regulator was capable of providing different voltage levels, only one power level was used throughout the T-39A experiment. As with the results from the F-15 FTF, the T-39A drag reduction was a strong function of the free-stream Reynolds number. Figure 18 shows that the same trend observed in the F-15B FTF experiment: boundary layer heating is most effective at lower Reynolds numbers.

The effect of the number of banks heated was also measured. Much like the low speed wind tunnel results, more heaters are more effective, but there is a diminishing rate of return for adding more elements. Figure 19 shows data taken at a Mach number of 0.70 and an altitude of 30,000 feet. As the wind tunnel test showed earlier, cutting the number of heater

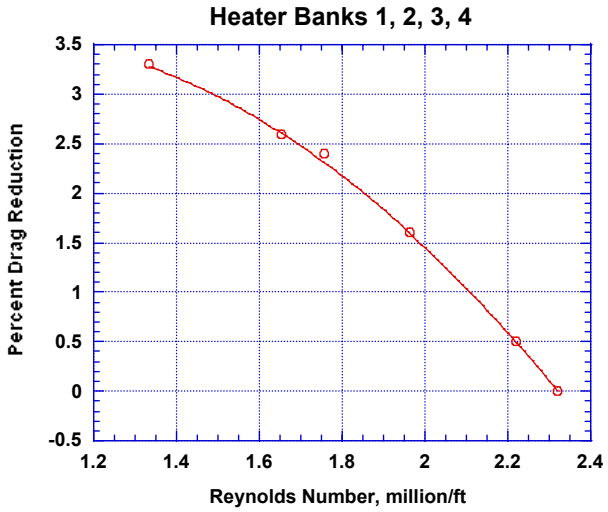

Figure 18: Effect of Reynolds number, T-39A

elements in half (and therefore the power required), reduces the benefit by much less than half. When only one bank was used, nearly all the benefit was lost. There remains a large potential benefit from the proper optimization of the heater bank arrangement.

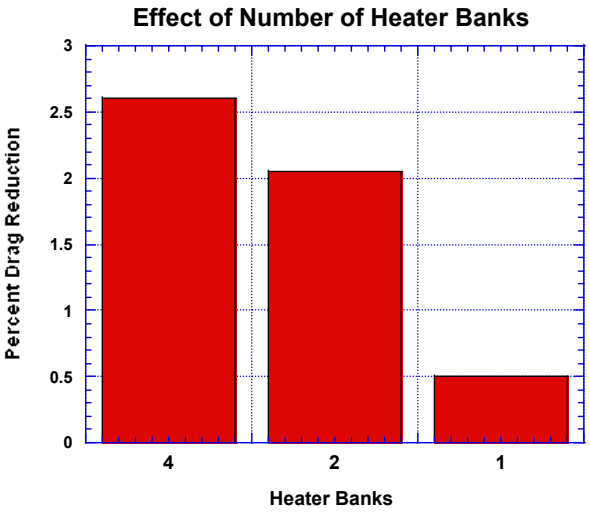

Figure 19: Effectiveness of Heater Length

CONCLUSIONS

Boundary layer heating was found most effective at low Reynolds number flight conditions. This was due to the reduced heat transfer rates and subsequently higher surface temperatures. While the surface temperatures obtained in the T-39A test at higher speeds did not appear to provide substantial drag reduction, it is believed that a more efficient heating method could be effective at these flight conditions.

The low speed wind tunnel test and the F-15B FTF experiment measured skin friction changes on bodies where skin friction accounted for nearly 100% of all drag. The T-39A test measured the gross drag of a vehicle where only approximately 15-20% of the total drag comes from fuselage skin friction. In order for the total drag to have decreased by 3.3%, as in the 40,000 ft M = 0.70 case, the fuselage skin friction must have decreased by 16-22%. Figure 20 shows the results of all three experiments. For purposes of illustation, the T-39A data has been calculated assuming that the fuselage skin friction accounts for 18% of the total drag. While these three experiments had different boundary layer temperature ratios, Fig. 20 does show the general trend of increasing effectiveness with lower Reynolds number. If higher boundary layer temperatures are achieved, the curve will move upward.

While loading an aircraft full of batteries is clearly not a practical alternative, this work has shown that an effective heat source can provide significant drag savings through boundary layer heating. In addition, vehicles that operate at very low Reynolds numbers, such as very high altitude drones, may be able to benefit the most from this technique.

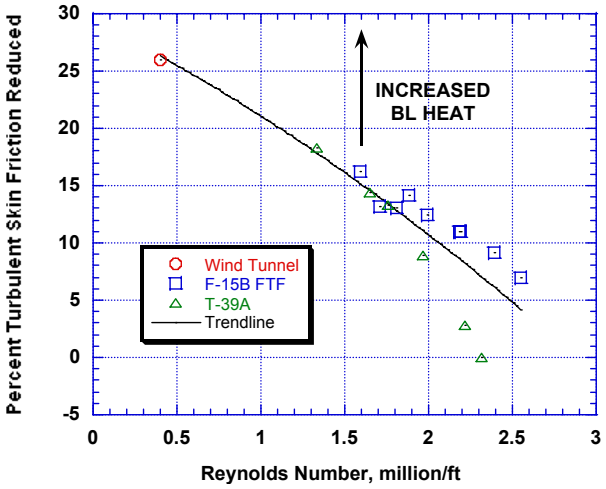

Figure 20: General Trend of Three Experiments

REFERENCES

1. Hoerner, S. F.; "Fluid-Dynamic Drag," Published by the Author, 1965.

2. Suárez, C. J., Ayers, B. F. and Malcolm, G. N.; "Force and Moment Measurements in a Flow Visualization Water Tunnel," AIAA Paper 94-0673, presented at the 32nd Aerospace Sciences Meeting, Reno, NV, January 1994.

3. Suárez, C. J. and Malcolm, G. N.; "Water Tunnel Force and Moment Measurements on an F/A-18," AIAA Paper 94-1802, presented at the 12th Applied Aerodynamics Conference, Colorado Springs, CO, June, 1994.

4. Lin, J. C.; Ash, R. L.; "Wall Temperature Control of Low-Speed Body Drag," Journal of Aircraft, Vol. 23, No. 1, January 1986.

5. Zuniga, F. A.; Anderson, B. T.; Bertelrud, A.; "Flight Test Results of Riblets at Supersonic Speeds," NASA Technical Memorandum 4387, 1992.

6. Covert, E. E.; "Thrust and Drag: Its Prediction and Verification," AIAA series Progress in Astronautics and Aeronautics, Volume 98, 1985

7. Pratt and Whitney Aircraft; "JT12 Military Turbojet Engine Installation Handbook," Revised August, 1964.

8. Rattenborg, J., Andersen, K.; "Performance Project: T-39A Sabreliner," National Test Pilot School, 1993.

9. Roberts, S. C.; "Light Aircraft Performance for Test Pilots and Flight Test Engineers," Flight Research, Inc., Mojave, CA 1980.